



Universiteit
Leiden
The Netherlands

Effects of heavy fields on inflationary cosmology

Ortiz, P.

Citation

Ortiz, P. (2014, September 30). *Effects of heavy fields on inflationary cosmology*. *Casimir PhD Series*. Retrieved from <https://hdl.handle.net/1887/28941>

Version: Not Applicable (or Unknown)

License: [Leiden University Non-exclusive license](#)

Downloaded from: <https://hdl.handle.net/1887/28941>

Note: To cite this publication please use the final published version (if applicable).

Cover Page



Universiteit Leiden



The handle <http://hdl.handle.net/1887/28941> holds various files of this Leiden University dissertation.

Author: Ortiz, Pablo

Title: Effects of heavy fields on inflationary cosmology

Issue Date: 2014-09-30

Perturbative stability along the supersymmetric directions of the landscape

In this chapter we generalise the study of the perturbative stability of non-supersymmetric configurations in $\mathcal{N} = 1$ supergravity models with a spectator sector not involved in supersymmetry breaking. Motivated by the supergravity description of complex structure moduli in Large Volume Compactifications of type IIB-superstrings, we concentrate on models where the interactions are consistent with the supersymmetric truncation of the spectator fields, and we describe their couplings by a random ensemble of generic supergravity theories. We characterise the mass spectrum of the spectator fields in terms of the statistical parameters of the ensemble and the geometry of the scalar manifold. Our results show that the non-generic couplings between the spectator and the supersymmetry breaking sectors can stabilise all the tachyons which typically appear in the spectator sector before including the supersymmetry breaking effects, and we find large regions of the parameter space where the supersymmetric sector remains stable with probability close to one. We discuss these results about the stability of the supersymmetric sector in two physically relevant situations: non-supersymmetric Minkowski vacua, and slow-roll inflation driven by the supersymmetry breaking sector. For the class of models we consider, we have reproduced the regimes in which the KKLT and Large Volume Scenarios stabilise all supersymmetric moduli. We have also identified a new regime in which the supersymmetric sector is stabilised at a very robust type of dS minimum without invoking a large mass hierarchy.

5.1 Introduction

In the last decade, many promising cosmological models have been derived in the framework of string theory and supergravity in order to understand the mechanisms responsible for the present acceleration of the universe, and for inflation. The construction of those models is far from trivial, in particular due to the fact that the supergravity description typically involves hundreds of scalar fields, *the moduli*. Any cosmological model requires a good understanding of the effective scalar potential along all directions in field space, since any tachyonic instability can easily spoil their predictions. Instead of performing an exhaustive analysis involving all the fields, one can characterise the properties of the effective potential following a statistical treatment [207–216].

One particular method to characterise the properties of the landscape is to study random ensembles of generic four dimensional $\mathcal{N} = 1$ supergravity theories with a large number of fields, $N \gg 1$, where the couplings are treated as random variables [210–212, 217, 218]. This framework is known as *random supergravity*. Although a generic supergravity theory cannot capture the specific properties of the supergravity Lagrangians, these ensembles are expected to describe correctly the generic features of the landscape. In this framework it has been shown that the construction of viable cosmological models is very constrained. In particular, this method has been used to determine the probability of occurrence of dS minima of the scalar potential which could describe the present day accelerated expansion. It was proven in [211, 212] that, in the case of generic supergravity theories, only an exponentially small fraction of the total number of critical points are non-tachyonic, $P_{\min} \sim e^{-N^p}$, with p being a number of order one, and N the number of scalar fields of the supergravity theory. Similarly, the possibility of constructing viable models of inflation in the string landscape has also been considered in several works [217, 218], where it was argued that prolonged periods of inflation are very rare due to the large probability of encountering instabilities along the inflationary trajectory, and this favours small field inflationary models. The random supergravity approach is a powerful tool in those situations where there is very little information available about the effective low energy Lagrangian under study.

Interestingly enough, in the so-called *Large Volume Scenario* (LVS), numerical analyses of specific compactifications show that the probability that a de Sitter critical point of the potential is tachyon-free is rather close to unity [213–216]. This is already true when the number of fields is small, $N \sim 5$, and the probability *increases* as the number of fields becomes larger [215]. This is in contrast with the results of the random supergravity approach.

The underlying reason for this apparent contradiction between the random supergravity approach and the analysis of the effective potential in LVS, is

5.1. Introduction

the fact that the random supergravity approach does not take into account the structure of the effective supergravity Lagrangian, or in other words, the non-generic structure of the Kähler potential for this case. The main objective of the present work is to study a random supergravity theory which captures the essential features of the couplings in these theories. We will prove that taking into account very general properties of this type of Lagrangians, it is possible to reconcile the results of these two approaches regarding the existence of stable dS vacua, and indeed we find that for non-generic couplings that resemble LVS the probability of finding stable dS vacua is exponentially close to one. In addition, we will explore the predictions of this random supergravity theory regarding the stability of the supersymmetric sector during inflation.

The intuition that the different sectors of the theory — namely complex structure moduli/dilaton (supersymmetric) sector and the Kähler moduli (non-supersymmetric) sector — are decoupled from each other is a misconception of the standard two-step approach to moduli stabilisation and the construction of stable dS vacua [219–221]. The consistency of using a low energy effective action for the Kähler moduli obtained by the approximate supersymmetric truncation of the complex structure and dilaton fields has been extensively checked in the literature [184–187, 189, 222, 223]. However this does not imply that the two sectors are decoupled. As we have seen in the previous chapter, the masses of the truncated sector depend on the dynamical sector.

This point becomes very important when considering the stability of the supersymmetric sector. It is often assumed that, in order for these fields to remain non-tachyonic in the full model, it is necessary to stabilise them at a supersymmetric AdS minimum of the scalar potential before including the couplings to the non-supersymmetric sector and the supersymmetry breaking effects. In the present work we will prove that this is not necessarily the case. In particular, we will study the stability of non-supersymmetric configurations on generic supergravity theories including only chiral multiplets. For the proof it will be sufficient to consider the stability along the supersymmetry-preserving directions of field space. We will show that the condition that the supersymmetric sector must be stabilised at a minimum of the scalar potential before including supersymmetry breaking, is not sufficient in general to ensure the stability in of the full non-supersymmetric configuration, and moreover, we will argue that there are physically relevant situations, as in LVS, where this condition is not even necessary. As a consequence, stable non-supersymmetric configurations will correspond in general to saddle points, or even AdS maxima of the scalar potential in the supersymmetric limit, that is, before the spontaneous breaking of supersymmetry is included. This claim has been already confirmed by numerical analyses elsewhere [216].

Here we will analyse the stability of supersymmetric sectors in $\mathcal{N} = 1$

supergravity theories using the random supergravity techniques developed in [210–212]. Since it is not consistent to study a supersymmetric sector in isolation, that is, neglecting the remaining fields and the effects of supersymmetry breaking, we need to choose an appropriate framework to be able to implement the random supergravity approach. In particular, we will concentrate on supergravity models with couplings compatible with freezing one sector of the theory at a supersymmetric critical point of the potential, and in particular we will study models where the couplings are consistent with the *exact supersymmetric truncation* of a sector of the fields [177], as we did in the previous chapter. In a consistent supersymmetric truncation, the solutions to the equations of motion obtained after truncating the supersymmetric sector are also exact solutions to the equations of the full model, and moreover, supersymmetry is exactly preserved in the reduced theory.

We perform the stability analysis of the supersymmetric sector and derive a set of necessary conditions for the stability of non-supersymmetric configurations in $\mathcal{N} = 1$ supergravity models with no gauge interactions. This set of constraints is complementary to the ones studied in [194, 195, 224–227], which ensure the stability of the scalar potential along the sGoldstino direction, that is, along the direction of supersymmetry breaking. In these works the necessary condition was translated into a constraint on the geometry of the Kähler manifold, which was expressed in terms of the *holomorphic sectional curvature* at the extremum, $S[X] \equiv -R_{X\bar{X}X\bar{X}}$, and of the square of the Hubble parameter measured in units of the gravitino mass¹, $\gamma = V/3m_{3/2}^2 \simeq H^2/m_{3/2}^2$:

$$S[X] \geq -\frac{2}{3} \frac{1}{1 + \gamma}.$$

Here we will derive an analogous set of conditions which ensure the stability along the remaining directions orthogonal to the sGoldstino, or in other words, the supersymmetry-preserving directions. This set of constraints depends not only on the parameter γ and on the geometry of the Kähler manifold, but also on the spectrum of masses of the chiral fermions m_λ and on their derivatives along the sGoldstino direction $\partial m_\lambda / \partial X$. These constraints can be expressed as a bound on the curvature of the Kähler manifold at the extremum through the quantity $B[X, \lambda] = -R_{X\bar{X}\lambda\bar{\lambda}}$, known as the *holomorphic bisectional curvature*, along the directions defined by the sGoldstino ξ^X and the supersymmetric directions ξ^λ :

$$3(\gamma + 1) B[X, \lambda] \geq -(m_\lambda \pm 1)(m_\lambda \pm (3\gamma + 1)) \mp \sqrt{3(\gamma + 1)} \frac{\partial m_\lambda}{\partial X}.$$

In addition, we shall discuss examples where this set of constraints is not only necessary, but also sufficient to ensure the stability along the supersymmetric directions at the critical point, and prove that the type of couplings which allow this

¹The correspondence between γ and b in the previous chapter is given by $b = 3\gamma$.

5.2. Aspects of $\mathcal{N} = 1$ supergravity

situation arise naturally when the model is consistent with the supersymmetric truncation of one sector of the moduli space. Moreover, we will show that field configurations minimising the gravitino mass along the supersymmetric directions are the best candidates to remain stabilised for arbitrary values of the uplifting γ . This could already be seen from the stability diagram presented in the previous chapter.

However, without some knowledge about the spectrum of fermion masses of the supersymmetric sector, these conditions are still not very informative. Following [209–212], we will adopt a statistical approach under the assumption that the supersymmetric sector contains a large number of fields. In particular, we will consider models where the couplings are consistent with the supersymmetric truncation of one sector of the theory, and we will describe the supersymmetric sector by a random ensemble of supergravity theories. Proceeding in this way, we find the mass spectrum of the fermions using random matrix theory techniques, and we shall derive constraints on the geometry of the Kähler manifold, expressed as bounds on the bisectional curvature $B[X, \lambda]$. These bounds will depend in general on the statistical parameters defining the random ensemble of supergravity theories, such as the standard deviation of the fermion masses, which sets the typical ratio of the mass of the heaviest fermion to the gravitino mass.

In the following, for the sake of simplicity and given the limitations of space, I present the main ingredients and key arguments that we used in order to get our results, and further details can be found in the original work [4].

5.2 Aspects of $\mathcal{N} = 1$ supergravity

Already in section 1.4.1 and in chapter 4 we reviewed the basic properties of the scalar potential and its critical points. The class of supergravity actions we study in the present work only involve complex scalar fields ξ^I and their superpartners, the Weyl fermions χ^I (chiral multiplets with no gauge interactions). The fields are labeled with the index I running in $I = 1, \dots, N$ for N chiral multiplets.

At critical points ξ_0 where supersymmetry is spontaneously broken, the gradient of the Kähler function $G_I|_{\xi_0}$ defines a direction in field space known as the *sGoldstino direction*. The sGoldstino corresponds to the supersymmetric partner of the would-be Goldstone fermion associated to broken supersymmetry. We will also describe this direction in terms of the unit vector z_X with coordinates

$$z_{X,I} = \frac{G_I}{\sqrt{G_K G^K}}. \quad (5.2.1)$$

From the supersymmetry transformations (1.4.6) it follows that a homogeneous bosonic field configuration ξ_0 where supersymmetry is unbroken must necessarily

satisfy the set of necessary conditions

$$G_I|_{\xi_0} = 0, \quad \text{for all } I = 1, \dots, N. \quad (5.2.2)$$

Actually, it is easy to check that supersymmetric configurations are also critical points of the scalar potential, see Eqs. (1.4.12) and (1.4.13) in section 1.4.2, and thus they are called *supersymmetric critical points*. Due to the form of the scalar potential (1.4.5), supersymmetric critical points are always AdS:

$$V|_{\xi_0} = -3e^G < 0, \quad (5.2.3)$$

except in those cases where the superpotential vanishes, for which they are Minkowski vacua, $V|_{\xi_0} = 0$.

5.2.1 The structure of the Hessian

For completeness and in order to establish our notation, let us review some aspects of the mass matrix already explained in section 4.2.1. In order to determine the stability properties of an extremum of the scalar potential, we need to study the eigenvalue spectrum of the corresponding Hessian,

$$\mathcal{H} = \begin{pmatrix} \nabla_I V_J & \nabla_I V_J \\ \nabla_I V_J & \nabla_I V_J \end{pmatrix}, \quad (5.2.4)$$

which determines the squared-masses of the scalar fields at Minkowski and de Sitter critical points. In this subsection we will describe the different contributions of the Hessian and will relate them to the masses of the fermions and to the geometry of the Kähler manifold.

After using the stationarity conditions (1.4.12), the second covariant derivatives of the scalar potential at the extremum ξ_0 of V read²

$$\begin{aligned} \nabla_I V_J &= (G_{IJ} - G_I G_J) V + e^G \left[G^{K\bar{L}} (\nabla_K G_I) (\nabla_L G_J) + G_{IJ} - R_{IJKL} G^K G^{\bar{L}} \right], \\ \nabla_I V_J &= (\nabla_I G_J - G_I G_J) V + e^G \left[2\nabla_I G_J + G^K \nabla_K \nabla_I G_J \right]. \end{aligned} \quad (5.2.5)$$

In these expressions it is straightforward to identify the mass of the gravitino $m_{3/2}$ and the mass matrix of the chiral fermions M_{IJ} :

$$m_{3/2} \equiv e^{G/2}, \quad M_{IJ} \equiv e^{G/2} \nabla_I G_J. \quad (5.2.6)$$

To simplify the notation, in what follows we will measure all the masses and energies in units of the gravitino mass, thus we perform the rescaling

$$\mathcal{H} \rightarrow m_{3/2}^2 \mathcal{H}, \quad \text{and} \quad M_{IJ} \rightarrow m_{3/2} M_{IJ}. \quad (5.2.7)$$

²To make contact to the notation of [83, 84], note that at any supersymmetric critical point ξ_0 the covariant derivatives and the regular derivatives of $G(\xi, \bar{\xi})$ coincide.

5.3. Necessary conditions for metastability

Similarly, we will parameterise the expectation value of the scalar potential at an extremum ξ_0 by the quantity:³

$$\gamma \equiv \frac{V}{3m_{3/2}^2} \simeq \frac{H^2}{m_{3/2}^2}, \quad (5.2.8)$$

which is essentially the square of the Hubble parameter H in units of the gravitino mass. The structure of the Hessian becomes particularly clear when we choose the fields ξ^I so that they have canonical kinetic terms at the critical point, i.e. $G_{I\bar{J}}|_{\xi_0} = \delta_{I\bar{J}}$. Moreover, we will require that one of the axis of the local frame points along the sGoldstino direction, i.e. $G_I \equiv G_X \delta_{IX}$, this is the so-called *sGoldstino basis*. In these coordinates it is straightforward to show that the Hessian reads⁴

$$\mathcal{H} = (\mathcal{M} + \mathbb{1})(\mathcal{M} + (3\gamma + 1)\mathbb{1}) + \sqrt{3(\gamma + 1)} \nabla_X \mathcal{M} - 3(\gamma + 1)\mathcal{R} - 9\gamma(\gamma + 1)\mathcal{P}_X. \quad (5.2.9)$$

Here \mathcal{M} and $\nabla_X \mathcal{M}$ are the (rescaled) fermion mass matrix and its derivative along the sGoldstino direction written in the $2N$ -vector notation, \mathcal{R} is a matrix built from the components of the Riemann tensor, and \mathcal{P}_X is the projector along the sGoldstino direction:

$$\mathcal{M} = \begin{pmatrix} 0 & \nabla_I G_{\bar{J}} \\ \nabla_{\bar{I}} G_{\bar{J}} & 0 \end{pmatrix}, \quad \mathcal{R} = \begin{pmatrix} R_{X\bar{X}I\bar{J}} & 0 \\ 0 & R_{\bar{X}X\bar{I}J} \end{pmatrix}, \quad \mathcal{P}_X = \begin{pmatrix} \delta_{IX}\delta_{\bar{J}\bar{X}} & \delta_{IX}\delta_{JX} \\ \delta_{\bar{I}\bar{X}}\delta_{\bar{J}\bar{X}} & \delta_{\bar{I}\bar{X}}\delta_{JX} \end{pmatrix}. \quad (5.2.10)$$

For convenience, we will define the following shorthand to refer to the first term of the Hessian in (5.2.9):

$$\mathcal{H}_\gamma \equiv (\mathcal{M} + \mathbb{1})(\mathcal{M} + (3\gamma + 1)\mathbb{1}). \quad (5.2.11)$$

5.3 Necessary conditions for metastability

In this section we will present our approach to characterise the perturbative stability of a consistently decoupled supersymmetric sector. We will derive a set of necessary conditions that should be satisfied by any homogeneous field configuration free of tachyons, and we will discuss some of their implications. As we shall show, our results can be applied both to the study of the perturbative stability of critical points of the scalar potential, or to analyse the viability of inflationary models which include a set of spectator fields not directly involved in the inflationary dynamics or supersymmetry breaking.

³Recall that b in chapter 4 equals 3γ .

⁴We also have the freedom to choose the sGoldstino vector to be real, which results into $G_X = \sqrt{3(\gamma + 1)}$.

For a Minkowski or de Sitter field configuration to be metastable, all the eigenvalues of the Hessian matrix (5.2.9) have to be positive. Since a generic expression of the eigenvalues in terms of G and its derivatives is too involved, we follow a different strategy. In the series of papers [194, 195, 224–227] they made use of the following observation: if the Hessian is positive definite, so it is its projection along any vector $Z = (z, \bar{z})^T$:

$$\langle Z, \mathcal{H} Z \rangle \geq 0. \quad (5.3.1)$$

In particular, the authors of [194, 195, 224–227] studied the condition obtained from imposing this requirement along the (complex) sGoldstino directions

$$Z_{+X} = \frac{1}{\sqrt{2}} \begin{pmatrix} z_X \\ z_{\bar{X}} \end{pmatrix} \quad \text{and} \quad Z_{-X} = \frac{i}{\sqrt{2}} \begin{pmatrix} z_X \\ -\bar{z}_X \end{pmatrix}. \quad (5.3.2)$$

As was discussed in detail in [194, 195], the corresponding constraint (5.3.1) is particularly restrictive due to the stationarity conditions, which imply that the vectors $Z_{\pm X}$ are eigenvectors of the fermion mass matrix \mathcal{M} :

$$\mathcal{M} Z_{\pm X} = \mp(3\gamma + 1) Z_{\pm X}. \quad (5.3.3)$$

Combining the necessary conditions associated to the vectors $Z_{\pm X}$, it is possible to find a restriction on the geometry of the Kähler manifold which, when expressed in terms of the *sectional curvature* $S[X] \equiv -R_{X\bar{X}X\bar{X}}$, reads:

$$S[X] \geq -\frac{2}{3} \frac{1}{1 + \gamma}. \quad (5.3.4)$$

In the present section we will derive a set of complementary conditions obtained when considering the other $2N - 2$ real directions orthogonal to the sGoldstino, that is, those preserving supersymmetry. Thus, in the rest of our analysis the term \mathcal{P}_X in (5.2.9) will always be absent.

5.3.1 Metastability conditions

To characterise the eigenvalue spectrum of the Hessian it is convenient to work in a local frame where the fermion mass matrix \mathcal{M} is diagonal, since in this basis the term \mathcal{H}_γ of the Hessian (5.2.9) is also diagonal. Due to the special structure of \mathcal{M} , it is possible to show that it has $2N$ real eigenvalues arranged in pairs of the form^{5,6}

$$\mathcal{M} Z_{\pm\lambda} = \pm m_\lambda Z_{\pm\lambda}, \quad \text{with} \quad \lambda = 1, \dots, N. \quad (5.3.5)$$

⁵The details of the diagonalisation can be found in Appendix C.

⁶Note the change of notation with respect to [3, 83, 84], where the masses of the fermions were denoted by $|x_\lambda| \equiv m_\lambda$.

5.3. Necessary conditions for metastability

The corresponding normalised eigenvectors are given by $Z_{+\lambda} = \frac{1}{\sqrt{2}}(z_\lambda, \bar{z}_\lambda)^T$ and $Z_{-\lambda} = \frac{1}{\sqrt{2}}(iz_\lambda, -i\bar{z}_\lambda)^T$, where z_λ solves

$$M \bar{z}_\lambda = m_\lambda z_\lambda, \quad (5.3.6)$$

and we choose $m_\lambda \geq 0$. Since M is symmetric, we can always find a set of orthonormal vectors z_λ which satisfy the previous equation. Indeed, after requiring the fields to have canonical kinetic terms, it is still possible to redefine them using a unitary transformation of the form $\tilde{\xi} = \xi U$. Performing these transformations we can bring the matrix M to a diagonal form $M = UDU^T$, where U is unitary and $D = \text{diag}(m_\lambda)$, with $m_\lambda \in \mathbb{R}^+$. This result, known as Takagi's factorisation, applies to any complex symmetric matrix, and the eigenvectors z_λ can be read from the columns of the unitary matrix $U_{I\lambda} = z_{\lambda,I}$. Note that this diagonalisation is also consistent with the choice of the sGoldstino basis since the vectors $Z_{\pm X}$ associated to the sGoldstino direction are also eigenvectors of the matrix \mathcal{M} , (5.3.3). The particular eigenvalue m_X is related to the unphysical Goldstone fermion of broken supersymmetry, and thus it does not have the interpretation of a mass. The rest of the parameters m_λ , with $\lambda = 1, \dots, N-1$, determine the mass spectrum of the chiral fermions χ^I .

In general, the contributions to the Hessian proportional to $\nabla_X \mathcal{M}$ and \mathcal{R} will not be diagonal in the basis formed by $Z_{\pm\lambda}$, but their diagonal elements in this frame

$$\langle Z_{\pm\lambda}, \nabla_X \mathcal{M} Z_{\pm\lambda} \rangle = \pm \frac{\partial m_\lambda}{\partial X}, \quad \langle Z_{\pm\lambda} \mathcal{R} Z_{\pm\lambda} \rangle = -B[X, \lambda], \quad (5.3.7)$$

have a simple physical interpretation. First, it can be shown that the parameters $\partial m_\lambda / \partial X$ are the derivatives of the fermion masses along the sGoldstino direction (see appendix C). Second, the set of $N-1$ quantities $B[X, \lambda] \equiv -R_{X\bar{X}\lambda\bar{\lambda}}$ are the so-called *bisectional curvatures* along the planes formed by the sGoldstino direction z_X and each of the eigenvectors z_λ , which has also been used to characterise the stability of the inflationary trajectory [86]. The viability of the studied models translates into constraints on the geometry of the Kähler manifold through the bisectional curvature.

In order to derive a set of simple necessary constraints, we will use the projection of the Hessian along all the $2N-2$ supersymmetric $Z_{\pm\lambda}$ directions, $\mu_{\pm\lambda}^2 \equiv \langle Z_{\pm\lambda}, \mathcal{H} Z_{\pm\lambda} \rangle$. Collecting the results above we find the following conditions for Minkowski and dS vacua:

$$\mu_{\pm\lambda}^2 = (m_\lambda \pm 1)(m_\lambda \pm (3\gamma + 1)) \pm \sqrt{3(\gamma + 1)} \frac{\partial m_\lambda}{\partial X} + 3(\gamma + 1) B[X, \lambda] \geq 0, \quad (5.3.8)$$

for all $\lambda = 1, \dots, N-1$. Similarly to [194, 195, 224–227], one can find a necessary condition which does not depend on the derivatives of the fermion masses by

adding together the quantities $\mu_{+\lambda}^2$ and $\mu_{-\lambda}^2$, which for $\gamma \geq 0$ reads

$$\mu_{+\lambda}^2 + \mu_{-\lambda}^2 \geq 0 \quad \implies \quad B[X, \lambda] \geq -\frac{m_\lambda^2 + 3\gamma + 1}{3(\gamma + 1)}. \quad (5.3.9)$$

In the case of AdS critical points, the requirement of stability implies that all the squared-masses of the scalar fields have to satisfy the Breitenlohner-Freedman bound [228], and therefore all the previous conditions have to be modified accordingly. For instance, taking into account that we work in units of the gravitino mass, the set of conditions (5.3.8) become

$$\mu_{\pm\lambda}^2 \geq \frac{3}{4} \frac{V(\xi_0)}{m_{3/2}^2} = \frac{9}{4}\gamma. \quad (5.3.10)$$

To understand the implications of the set of constraints (5.3.8) and their dependence on the different parameters of the theory, (the spectrum of fermion masses and their derivatives, the geometry of the Kähler manifold, and the supersymmetry breaking scale), we will now discuss them in two different contexts:

- First, we will analyse the metastability of supersymmetric critical points, where we recover known results. In that situation the parameters $\mu_{\pm\lambda}^2$ are the exact eigenvalues of the Hessian, and therefore the corresponding constraints (5.3.10) are both necessary and sufficient to guarantee the perturbative stability of the configuration.
- Second, we will discuss non-supersymmetric configurations, focusing on the perturbative stability of the fields preserving supersymmetry. This analysis is both applicable to the case when the field configuration represents a non-supersymmetric vacuum or when it is responsible for driving an inflationary phase. In the latter case, the perturbative stability of all the fields not related to the inflaton or the sGoldstino is a requirement for the viability of the model, since the presence of any large tachyonic instability would spoil the slow-roll conditions. Additionally, the masses of the non-inflating fields must remain larger than the Hubble parameter in order to avoid large isocurvature fluctuations, which are ruled out by the observations. Even if they remain sufficiently massive, if these fields deviate from geodesics, they might leave imprints in the CMB temperature spectra [1, 103].

Let us emphasise that in general the conditions (5.3.8,5.3.9) are necessary but cannot guarantee the perturbative stability along the supersymmetric directions of a non-supersymmetric configuration. However, as we shall discuss in later sections, there are interesting situations where these conditions become both necessary and sufficient. For instance, whenever the term \mathcal{H}_γ dominates over the rest of contributions to the Hessian, since then the quantities $\mu_{\pm\lambda}^2$ can be identified as the eigenvalues of the Hessian to first order in perturbation theory.

5.3. Necessary conditions for metastability

We shall leave the discussion of these cases for section 5.4.

For simplicity, in the following analyses we will assume that all the parameters involved in the constraints (5.3.8) are independent from each other and can be varied freely. More complicated situations are possible, for example when two or more of the parameters have a functional dependence on each other, but we will not consider them here.

5.3.2 Supersymmetric vacua and uplifting to dS

As we discussed above, supersymmetric critical points are AdS as long as the superpotential is non-zero, $W \neq 0$, and in particular they satisfy $\gamma = -1$. Therefore, the Hessian (5.2.9) is simply given by:

$$\mathcal{H} = (\mathcal{M} + \mathbb{1})(\mathcal{M} - 2\mathbb{1}) \implies \mu_{\pm\lambda}^2 = (m_\lambda \pm 1)(m_\lambda \mp 2) = (m_\lambda \mp \frac{1}{2})^2 - \frac{9}{4} \geq -\frac{9}{4}. \quad (5.3.11)$$

This implies that the Hessian is also diagonal in the basis that diagonalises \mathcal{M} , and therefore the parameters $\mu_{\pm\lambda}^2$ can be identified with the complete set of eigenvalues of \mathcal{H} . Then the set of conditions (5.3.10) are *necessary and sufficient*, and in addition they can be applied to all directions $Z_{\pm\lambda}$, with $\lambda = 1, \dots, N$, since there is no sGoldstino at supersymmetric critical points. From the eigenvalues (5.3.11) one can see what type of extremum the supersymmetric critical point ξ_0 is, namely:

$$\begin{aligned} m_\lambda > 2 \quad \text{for all } \lambda &\implies \text{local AdS minimum,} \\ m_\lambda < 1 \quad \text{for all } \lambda &\implies \text{local AdS maximum,} \end{aligned} \quad (5.3.12)$$

and any other combination corresponds to AdS saddle points ($m_\lambda = 1, 2$ give flat directions). However, supersymmetric critical points are always perturbatively stable regardless of the possible negative curvature of the potential, since they are AdS and the Breitenlohner-Freedman bound (5.3.10) is always satisfied, as can be seen from eq. (5.3.11).

As discussed in the introduction, supersymmetric vacua play an important role in the construction of de Sitter vacua in cosmological models. It is possible to engineer a dS vacuum by the *uplifting* of a supersymmetric AdS vacuum ξ_0 to dS, which consists in introducing a physical mechanism to break supersymmetry. Ideally, these mechanisms add a positive definite correction to the scalar potential δV_{uplift} , possibly field-dependent, so that the vacuum expectation value of V becomes positive at ξ_0^I ,

$$V = V_{\text{susy}}|_{\xi_0} + \delta V_{\text{uplift}}|_{\xi_0} \geq 0, \quad (5.3.13)$$

while the supersymmetric configuration is still a metastable critical point of the potential. In general, the supersymmetric field configuration ξ_0 is not a

critical point of the uplifting term δV_{uplift} , and thus the critical points of the final potential typically shift away from ξ_0 , or disappear completely. That is why in general one should ensure that the original supersymmetric critical point ξ_0 is a minimum, demanding all chiral fermions to have masses larger than twice the gravitino mass, cf. (5.3.12).

One of the aims of this work is to study the metastability of a supersymmetric sector embedded in a larger model where supersymmetry is already broken. As we shall see in section 5.6, in that case the constraint we just discussed is no longer necessary. In particular we will prove that a stable configuration of the embedded supersymmetric sector may correspond to any type of AdS critical point (even a saddle point or maximum) in the supersymmetric limit $\gamma \rightarrow -1$. In other words, the embedding of the supersymmetric sector in a larger model may turn an AdS maximum or a saddle point in the supersymmetric limit to a metastable configuration after supersymmetry breaking by other sector. The coupling between the embedded supersymmetric sector and the fields breaking supersymmetry can be seen as a non-generic type of F-term uplifting mechanism, like those studied in [83, 84].

5.3.3 Non-supersymmetric configurations

In the present subsection we will analyse the set of constraints (5.3.8) in the case when the field configuration is non-supersymmetric. As we mention above, we shall consider both the case where the configuration is an extremum of the scalar potential, and where the vacuum energy of the fields is driving an inflationary phase. In order to proceed we analyse the different contributions to the Hessian separately: first we will discuss the term depending on the fermion mass matrix \mathcal{H}_γ , and then we will characterise the effect of including the contributions associated to the derivatives of the fermions masses $\nabla_X \mathcal{M}$, and the curvature of the Kähler manifold, \mathcal{R} .

Dependence on the fermion masses, $\mathcal{H} = \mathcal{H}_\gamma$

We begin with the simplest case where \mathcal{H}_γ is the only non-zero contribution to the Hessian:

$$\nabla_X \mathcal{M} = \mathcal{R} = 0 \quad \implies \quad \mathcal{H} = \mathcal{H}_\gamma = (\mathcal{M} + \mathbb{1})(\mathcal{M} + (3\gamma + 1)\mathbb{1}). \quad (5.3.14)$$

Then, as in the case of supersymmetric critical points, the Hessian is diagonal in the basis of eigenvectors $Z_{\pm\lambda}$ of the fermion mass matrix, and the quantities $\mu_{\pm\lambda}^2$ can be identified with the eigenvalues of \mathcal{H} , which read:

$$\mu_{\pm\lambda}^2 = (m_\lambda \pm 1)(m_\lambda \pm (3\gamma + 1)) = \left(m_\lambda \pm \frac{1}{2}(3\gamma + 2)\right)^2 - \frac{9}{4}\gamma^2. \quad (5.3.15)$$

Therefore, the stability of the configurations along the supersymmetric directions is entirely determined by the fermion mass spectrum m_λ and the parameter γ .

5.3. Necessary conditions for metastability

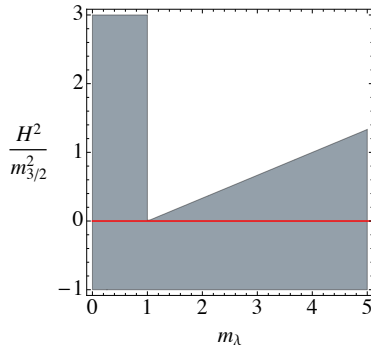


Figure 5.1 – Stability diagram for a Hessian of the form (5.3.14), with $\partial_X \mathcal{M} = \mathcal{R} = 0$. In this case the conditions (5.3.8) are both necessary and sufficient, and the shaded area represents the region of parameter space where they are satisfied. Configurations which minimise the gravitino mass $m_{3/2}^2 = e^G$ ($m_\lambda < 1$) remain stable for arbitrary large values of the parameter $\gamma \gg 1$.

Since all the eigenvalues of the Hessian are bounded below by $-\frac{9}{4}\gamma^2$ it follows that, when the configuration is an AdS critical point, $\gamma \in [-1, 0)$, these eigenvalues always satisfy the Breitenlohner-Freedman bound (5.3.10), and thus it is always stable. However, if the configuration is either Minkowski or de Sitter ($\gamma \geq 0$), stability demands

$$\mu_{\pm\lambda}^2 \geq 0 \quad \implies \quad m_\lambda < 1 \quad \text{or} \quad m_\lambda > 3\gamma + 1 \quad \text{for all } \lambda. \quad (5.3.16)$$

Thus, in Minkowski vacua ($\gamma = 0$) the supersymmetric sector is always metastable, possibly with flat directions if one or more of the fermion masses equals the gravitino mass, $m_\lambda = 1$. An interesting consequence for de Sitter configurations (either a vacuum or at a point of the inflationary trajectory) is that, if all fermion masses are smaller than the gravitino mass, i.e. $m_\lambda < 1$, the supersymmetric sector remains tachyon-free for arbitrary large values of the cosmological constant. Conversely, if the fermion spectrum contains any mass larger than $m_{3/2}$, the critical point will always become unstable for sufficiently large values of the Hubble parameter. These results are illustrated in Fig. 5.1, which shows the stability diagram of a non-supersymmetric configuration along a direction orthogonal to the sGoldstino. The horizontal axis is related to the mass of the corresponding fermionic partner m_λ , and the quantity on the vertical axis is the parameter γ . In the diagram, the perturbatively stable configurations are represented by the grey shaded area.

This simple example already illustrates the claim made in the previous subsection: in general, the condition $m_\lambda > 2$ necessary for a supersymmetric critical point to be a minimum, is neither necessary or sufficient when the supersymmetric sector is embedded in a larger model. The special structure of the Hessian

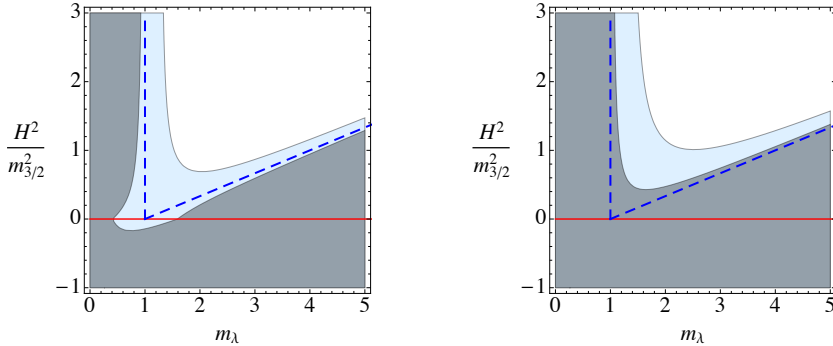


Figure 5.2 – Stability diagram associated to the spectrum given by equation (5.3.8). Coloured areas show, for different choices of parameters, the regions where the stability conditions are satisfied, while in the white area we would have tachyons. *LEFT*: $\partial m_\lambda/\partial X = 0.2$, with $B[X, \lambda] = 0$ (grey area) and $B[X, \lambda] = 0.3$ (light blue area). *RIGHT*: $\partial m_\lambda/\partial X = -0.2$, with $B[X, \lambda] = 0$ (grey area), and $B[X, \lambda] = 0.3$ (light blue area). The dashed line represents the constraints in the case $B[X, \lambda] = \partial m_\lambda/\partial X = 0$, showed in figure 5.1.

discussed in this example arises naturally in models of F-term uplifting where some heavy moduli are truncated while preserving supersymmetry [83, 84]. In the context of inflation this type of couplings have also been considered in [3], see chapter 4. We discuss more about this class of models in sections 5.4 and 5.6.

Dependence on the fermion mass derivatives and the curvature

In general, when the terms $\partial_X \mathcal{M}$ and \mathcal{R} are taken into account, the Hessian will not be diagonal in the basis formed by the vectors $Z_{\pm\lambda}$, and the set of necessary conditions (5.3.8) will not be sufficient to ensure the stability of the critical point.

Let us first focus on the contribution coming from the term in the Hessian proportional to the derivative of the fermions mass matrix $\nabla_X \mathcal{M}$, while keeping the curvature term set to zero $\mathcal{R} = 0$. In Fig. 5.2, focusing on the grey regions, we have represented the region of parameter space satisfying the stability conditions (5.3.8) for a particular direction in field space z_λ (shaded grey area) setting two different constant values of the fermion mass derivatives, $\partial m_\lambda/\partial X = 0.2$ (left plot) and $\partial m_\lambda/\partial X = -0.2$ (right plot), and with a zero bisectonal curvature $B[X, \lambda] = 0$. Since these conditions are in general necessary but not sufficient, a field configuration located in the grey shaded region is not necessarily stable, but those out of the shaded area will definitely contain one or more tachyonic directions in the spectrum. Note that when the derivatives of the fermion masses

5.3. Necessary conditions for metastability

satisfy

$$\left. \frac{\partial m_\lambda}{\partial X} \right|_{\text{opt}} = -\frac{3\gamma + 2}{\sqrt{3(\gamma + 1)}} m_\lambda, \quad (5.3.17)$$

the two parameters $\mu_{\pm\lambda}^2$ become equal, and both constraints (5.3.8) reduce to the less restrictive condition (5.3.9). Therefore, in the case of dS and Minkowski configurations ($\gamma \geq 0$), as the derivatives of the fermion masses approach this optimum value, the stability constraints on the fermion masses m_λ and the parameter γ become milder, as observed in the diagrams.

The effect of having a non-zero \mathcal{R} is simpler to analyse. The set of necessary conditions (5.3.8) clearly favour positive values for the bisectonal curvature $B[X, \lambda] > 0$. We can check that this is indeed the case in the plots of Fig. 5.2, where we have displayed the region of parameter space satisfying the stability conditions (5.3.8) for two different constant values of the bisectonal curvature, $B[X, \lambda] = 0$ (grey area), and $B[X, \lambda] = 0.3$ (light blue area).

When the Hubble scale is large compared to any of the fermion masses, $H \gg m_{3/2}$ and $H \gg m_\lambda m_{3/2}^7$, the bisectonal curvatures play a fundamental role determining the stability of the inflationary trajectory. In that limit (keeping $\partial m_\lambda / \partial X$ fixed) the range of fermionic masses where the field configuration is free of tachyons is

$$0 \leq m_\lambda \lesssim 1 + B[X, \lambda]. \quad (5.3.18)$$

Then, when the bisectonal curvature is zero, we recover the limit discussed above and only configurations where the largest mass of the chiral fermions satisfies $m_\lambda|_{\text{max}} < 1$, remain stable for arbitrarily large values of γ . However, positive values improve the stability, as shown by the light blue regions of Fig. 5.2, and negative values of the bisectonal curvature shrink the range of fermion masses compatible with stable dS configurations. Actually, when $B[X, \lambda] < -1$, the field associated to the direction z_λ always becomes tachyonic for sufficiently large values of the Hubble parameter, $\gamma \gg 1$, and therefore the corresponding field configuration is necessarily unstable.

These constraints are of interest both for the construction of de Sitter vacua with small cosmological constant $\gamma \approx 0$ (as in the present vacuum), and for models of inflation, to study the stability of the supersymmetric sector along the inflationary trajectory. The study of the viability of inflationary models using the presented constraints deserves further consideration and we will report on it in a future publication. We will now start with the stability analysis of consistently decoupled sectors, focusing on those models where they only act as spectators both in supersymmetry breaking and inflation.

⁷Recall that we measure the chiral fermion masses m_λ in units of the gravitino mass, $m_{3/2}$.

5.4 Modeling the supersymmetric sector

Having presented the main tool for our analysis, that is, the set of constraints (5.3.8), we now turn to the problem at hand: the study of the perturbative stability of a decoupled supersymmetric sector, such as the complex structure moduli in the KKLT constructions, and Large Volume Scenarios of Type IIB flux compactifications [219–221]. Motivated by these scenarios, where stabilisation of the complex structure moduli can be studied using a statistical treatment [209–212], we will focus on theories where the supersymmetric sector contains a large number of fields, and we will characterise the couplings using a statistical description. On the one hand, we will require the interactions of the model to be consistent with the *exact supersymmetric truncation* of the decoupled sector (section 5.4.1), and on the other hand we will assume that the couplings of the supersymmetric sector are generic and can be treated as random variables. In particular we will characterise the spectrum of fermion masses of the supersymmetric sector m_λ , and their derivatives, $\partial m_\lambda / \partial X$, using standard techniques from random matrix theory (section 5.4.2).

5.4.1 Supersymmetric decoupling

As discussed previously and extensively in this thesis, integrating out a heavy sector in a consistent way is only possible in certain situations. The type of couplings between the integrated and surviving sectors which allow for the reduced theory to be approximately supersymmetric have been discussed extensively in the literature [82, 186, 187, 189].

The simplest way of satisfying these conditions is to require the couplings to be consistent with the *supersymmetric truncation* of the heavy sector [177]. In a consistent truncation of a given theory, the solutions of the reduced theory are *exact* solutions of the full theory. This type of constructions are interesting for our purposes because they enable us to study the perturbative stability of the truncated sector on its own. In addition, the truncated fields will remain on geodesic trajectories. In this sense we can say that the truncated sector is *supersymmetrically decoupled* from the fields in the reduced theory. Interestingly, it has been shown [188, 229] that the large volume limit of type IIB flux compactifications are a particular realisation of this class of models, and moreover, in that case the conditions (5.3.8) are not only necessary, but also sufficient to ensure the stability of the supersymmetric sector.

Let us consider a heavy supersymmetric sector with fields H^α and a light supersymmetry-breaking sector with fields L^i . We have seen that in order for the truncated fields to preserve supersymmetry regardless of the configuration of the surviving sector L^i , the Kähler function has to satisfy the following set of

5.4. Modeling the supersymmetric sector

constraints:

$$G_\alpha(H_0, \bar{H}_0, L, \bar{L}) = 0 \quad \text{for all} \quad L^i \quad \text{and} \quad \alpha = 1 \dots N_h. \quad (5.4.1)$$

Since the equations (5.4.1) must hold for any value of the light fields L^i , the couplings between the two sectors are very constrained. Taking derivatives with respect to the coordinates L^i and $L^{\bar{i}}$ we find the following implications:

$$G_{i\alpha}(H_0, \bar{H}_0, L, \bar{L}) = 0, \quad R_{i\bar{j}k\bar{\alpha}} = 0, \quad (5.4.2)$$

$$M_{i\alpha}|_{H_0} = 0, \quad \nabla_X M_{i\alpha}|_{H_0} = 0. \quad (5.4.3)$$

The previous conditions imply that the Hessian itself must be block diagonal in the two sectors:

$$\mathcal{H} = \mathcal{H}_h \oplus \mathcal{H}_l. \quad (5.4.4)$$

Therefore, as we anticipated at the beginning of the section, if the couplings are compatible with the consistent truncation the supersymmetric sector, it is consistent to study the perturbative stability of the supersymmetric sector independently of the sector surviving the truncation, i.e. it is sufficient to consider the block of the Hessian \mathcal{H}_h :

$$\mathcal{H}_h = (\mathcal{M}_h + \mathbb{1})(\mathcal{M}_h + (3\gamma + 1)\mathbb{1}) + \sqrt{3(\gamma + 1)} \nabla_X \mathcal{M}_h - 3(\gamma + 1)\mathcal{R}_h. \quad (5.4.5)$$

In the following, we consider models with a supersymmetrically decoupled sector in the sense described above, focusing on the stability of the configuration defining the truncation, H_0^α , along the supersymmetric directions H^α .

5.4.2 Statistical description

Since the fine details of this subsection are not essential for the understanding of our results, we will review the main facts and concepts, and refer to the reader to the original work [4] for further details. In order to study the perturbative stability of the supersymmetrically decoupled sector, we need to characterise the eigenvalue spectrum of the fermion mass matrix \mathcal{M}_h and the properties of its derivative $\nabla_X \mathcal{M}_h$. At a generic point of the reduced theory, where $H^\alpha = H_0^\alpha$, these matrices read

$$\mathcal{M}_h = \begin{pmatrix} 0 & M_{\alpha\beta} \\ \bar{M}_{\bar{\alpha}\bar{\beta}} & 0 \end{pmatrix}, \quad \nabla_X \mathcal{M}_h = \begin{pmatrix} 0 & \nabla_X M_{\alpha\beta} \\ \nabla_{\bar{X}} \bar{M}_{\bar{\alpha}\bar{\beta}} & 0 \end{pmatrix}, \quad (5.4.6)$$

where the tensors $M_{\alpha\beta} = \nabla_\alpha G_\beta$ and $\nabla_X M_{\alpha\beta} = \nabla_X (\nabla_\alpha G_\beta)$ will depend in general on the configuration H_0^α and on the light fields L^i . In realistic scenarios with a large number of fields, it is more practical to follow the methods proposed by Denef and Douglas [209, 210] and later developed in [211, 212], who use a statistical approach. Indeed, treating the components of the tensors $M_{\alpha\beta}$ and $\nabla_X M_{\alpha\beta}$ as random variables, makes possible to characterise the properties of the matrices (5.4.6) using random matrix theory techniques (see [230]).

Probability distribution of the couplings

Following [211, 212], we assume that the random variables $M_{\alpha\beta} = M_{\beta\alpha}$ are characterised by a unique probability distribution Ω , with zero mean and standard deviation σ for $\alpha \neq \beta$ and $\sqrt{2}\sigma$ for $\alpha = \beta$:

$$M_{\alpha\beta} \in \Omega(0, \sigma) \quad \text{if } \alpha < \beta, \quad \text{and} \quad M_{\alpha\alpha} \in \Omega(0, \sqrt{2}\sigma). \quad (5.4.7)$$

Note that the corresponding joint probability distribution is invariant under supersymmetry and Kähler transformations, and diffeomorphisms on the Kähler manifold. In the limit where the size of the matrices is very large, i.e. large number of H^α fields, the results we will now present do not depend on any higher moments of the distribution Ω .

The quantities in the Hessian (5.4.5) associated to the supersymmetry breaking sector, i.e. γ and the gravitino mass $m_{3/2}$, will be regarded as parameters and studied in a case by case basis. Moreover, following the works in [207–210] we also assume that the geometry of the Kähler manifold is also determined by the parent theory. Note that these quantities depend on the configuration H_0^α and on the light fields L^i , and therefore our predictions about the stability of the supersymmetric sector will depend on the distribution of the couplings, the geometry of the moduli space, and the supersymmetry breaking scale.

In the following, we bring a few results of random matrix theory to characterise the spectrum of masses of the fermions m_λ and their derivatives along the sGoldstino direction $\partial m_\lambda / \partial X$. We then incorporate them to the analysis of the perturbative stability of the supersymmetric sector through the constraints (5.3.8).

The Altland-Zimbauer CI-ensemble

The set of hermitian matrices with the same structure as (5.4.6), and random complex entries drawn from a probability distribution with the properties given in (5.4.7), form the so-called *Altland-Zimbauer* or *CI-ensemble*. Taking the distribution Ω to be gaussian, the joint probability density for the fermion masses m_λ is given by

$$f(m_1, \dots, m_{N_h}) = \mathcal{C} \exp \left(-\frac{1}{2\sigma^2} \sum_{\lambda=1}^{N_h} m_\lambda + \sum_{\lambda < \nu}^{N_h} \ln |m_\nu - m_\lambda| + \sum_{\lambda=1}^{N_h} \ln m_\lambda \right). \quad (5.4.8)$$

The spectrum of eigenvalues is characterised by the spectral density $\rho(m) dm$, which gives the average number of fermions with mass in the interval $[m, m + dm)$. When $N_h \rightarrow \infty$ the spectral density is closely related to the Wigner's semicircle

5.4. Modeling the supersymmetric sector

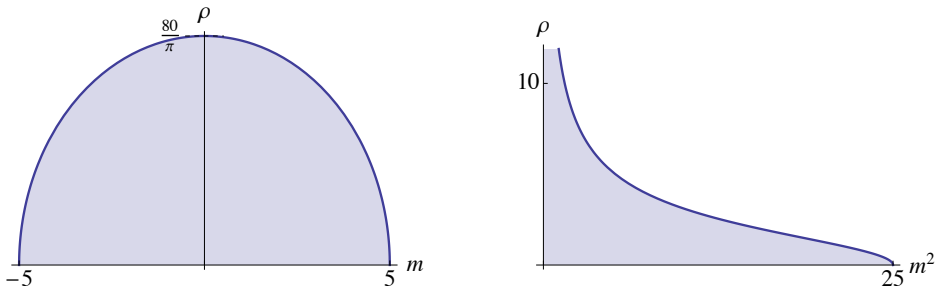


Figure 5.3 – Typical spectrum of fermion masses for $m_h = 5$ and $N_h = 100$. *LEFT:* The spectral density of the fermion mass matrix \mathcal{M} resembles Wigner’s semicircle law to leading order in $1/N$. *RIGHT:* The Marčenko-Pastur law gives the typical distribution for the square of the fermion masses m^2 .

law (SC) and reads:⁸

$$\rho_{\text{SC}}(m) = \frac{4N_h}{\pi m_h^2} \sqrt{m_h^2 - m^2}, \quad \rho_{\text{MP}}(m^2) = \frac{2N_h}{\pi m_h^2 m} \sqrt{m_h^2 - m^2}, \quad (5.4.9)$$

for $m \leq m_h$, and zero otherwise; where $m_h^2 = 4N_h\sigma^2$. For later convenience we have also written the distribution of the square of the fermion masses $\rho_{\text{MP}}(m^2) dm^2$, which is a particular case of the so-called Marčenko-Pastur law (MP) [231]. The fact that the spectral density (5.4.9) has a compact support in the large N_h limit does not imply that the probability of finding eigenvalues out from the specified range is zero. The previous expression only gives the *typical* spectrum of a large matrix from the CI-ensemble, but other *atypical* spectra are possible, with the cost of a suppressed probability (see appendix D). In fact, the chance of finding a mass fluctuation outside the boundaries $(0, m_h)$ is determined by the Tracy-Widom distribution [232], which predicts an exponential suppression of the form $e^{-aN_h^2}$.

The matrix $\nabla_X \mathcal{M}$ has similar symmetries and structure as \mathcal{M} , so we will assume that it can also be identified as an element from the CI-ensemble, but with a standard deviation σ_D . In the following, we analyse in detail the perturbative stability of the supersymmetrically truncated sector combining the constraints (5.3.8) with the statistical characterisation of the fermion mass spectrum just discussed.

⁸Actually the spectral density of the CI-ensemble presents a characteristic cleft of width $1/N_h$ near $m = 0$, where it behaves as $\rho_\chi(m) \sim m$, but we will neglect it as it becomes a subleading effects in the large N_h limit.

5.5 Statistics of supersymmetric vacua

Our starting point in this section are the results of section 5.3.2 regarding the character of AdS supersymmetric critical points. We now incorporate the statistical properties of the fermionic mass spectrum given by random matrix theory as discussed in the previous section, and we will review the results obtained in [212], stating that the probability of obtaining a tachyon-free vacuum after uplifting a supersymmetric AdS minimum to a stable dS is exponentially suppressed. In section 5.6 we will explore more general settings where the dS vacuum is constructed without requiring one sector of the fields to be stabilised at an AdS minimum, and show that the probability of the vacuum being tachyon-free can still be made of order one for certain values of the parameters which determine the distribution of the couplings and the geometry of the moduli space.

5.5.1 Eigenvalue spectrum of the Hessian

Supersymmetric AdS critical points are extrema of the Kähler function, and thus also of the gravitino mass (5.2.6). Moreover, at an AdS supersymmetric critical point, the Hessian of the scalar potential is closely related to the Hessian of the gravitino mass squared $m_{3/2}^2 = e^G$, which we shall denote by \mathcal{G} . After rescaling \mathcal{G} as in (5.2.7), and taking into account that the fields are canonically normalised, it can be shown that

$$\mathcal{G} = \mathbb{1} + \mathcal{M} \quad \Longrightarrow \quad \mathcal{H} = \mathcal{G}(\mathcal{G} - 3\mathbb{1}). \quad (5.5.1)$$

As was pointed out in [83, 84], this relation implies a one-to-one correspondence between the supersymmetric AdS maxima and the minima of the gravitino mass, which holds in full generality when gauge interactions are included [84]. To see this point, note that \mathcal{G} is also diagonal in the basis of $Z_{\pm\lambda}$ and the eigenvalues are given by

$$g_{\pm\lambda} = 1 \pm m_\lambda. \quad (5.5.2)$$

Thus, the gravitino mass is minimised in field configurations where all the fermion masses satisfy $m_\lambda < 1$, which corresponds precisely to supersymmetric AdS maxima (5.3.12).

Given the relation between \mathcal{H} and the Hessian of the gravitino mass, \mathcal{G} , let us start characterising the dependence of the spectral density of \mathcal{G} on the parameter m_h which determines the distribution of the fermion masses. It is easy to see that for $m_h < 1$, the fermion mass distribution is bounded to values smaller than the gravitino mass, and the eigenvalues of \mathcal{G} in (5.5.2) are positive, so those critical points correspond to minima of the gravitino mass. For $m_h > 1$ we have saddle points, and in the limit of very large standard deviations only half of the eigenvalues of \mathcal{G} are positive.

5.5. Statistics of supersymmetric vacua

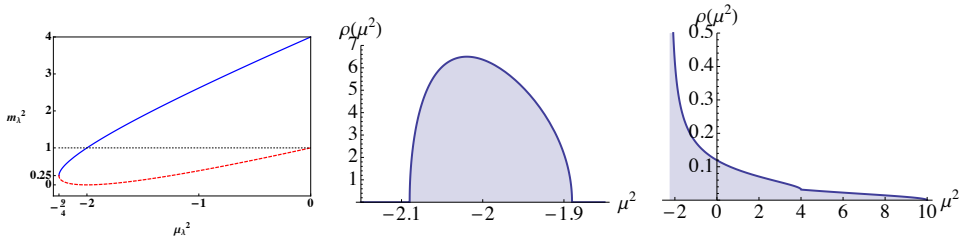


Figure 5.4 – *LEFT*: the two branches when inverting eq. (5.3.11). Note that for $m_h < 1$, that is, fermion masses smaller than the gravitino mass, we are in a supersymmetric AdS maximum. *CENTER*: probability distribution function in (5.5.4) for $m_h = 0.1$, where all modes are BF-allowed tachyons. *RIGHT*: probability distribution function in (5.5.4) for $m_h = 3$. In the plots the spectral densities are normalised to unity.

One can perform a similar analysis of the Hessian, which is given in terms of \mathcal{G} in (5.5.1). Then one can realise that for $m_h < 1$ the typical supersymmetric critical point is an AdS maximum, and as m_h becomes larger, the number of negative eigenvalues approaches zero asymptotically. It is interesting to note that saddle points are the dominant type of critical point for most values of m_h , and moreover, there is no finite value of the standard deviation of the fermions where the typical critical point is a supersymmetric minimum.

Let us now calculate the scalar mass spectrum for a typical supersymmetric critical point. The expression (5.3.11) relating the eigenvalues of the Hessian \mathcal{H} to the fermion masses can be used in combination with the Marčenko-Pastur law (5.4.9) to determine the typical spectral density of \mathcal{H} . First, expressing the square of the fermion masses in terms of the eigenvalues of the Hessian μ^2 , cf. eq. (5.3.11), we find a multiple-valued function with two branches, which we denote by $m_\pm^2(\mu^2)$, and are displayed in Fig. 5.4. Then, the contribution from each of the branches to the spectral density of \mathcal{H} reads simply:

$$\rho_{\text{MP}}(m_\pm^2) \left| \frac{dm_\pm^2}{d\mu^2} \right| = \Theta(m_h^2 - m_\pm^2) \frac{2}{\pi m_h^2} \sqrt{\frac{m_h^2 - m_\pm^2}{\mu^2 + \frac{9}{4}}}, \quad (5.5.3)$$

where m_\pm^2 should be understood as functions of μ^2 , and the Heaviside theta functions Θ are a reflection of the support of the Marčenko-Pastur distribution for each of the branches. The total eigenvalue density function, given the spectrum of the Hessian, can then be written as [212]:

$$\rho(\mu^2)d\mu^2 = \left[\rho_{\text{MP}}(m_+^2) \left| \frac{dm_+^2}{d\mu^2} \right| + \rho_{\text{MP}}(m_-^2) \left| \frac{dm_-^2}{d\mu^2} \right| \right] d\mu^2. \quad (5.5.4)$$

Illustrative examples of the distribution (5.5.4) are given in figure 5.4. In those plots we see that this spectrum interpolates between a shifted Wigner semicircle law for $m_h \rightarrow 0$, corresponding to AdS maxima, and a shifted version of the Marčenko-Pastur distribution for spectrum for $m_h \gg 1$, corresponding to supersymmetric critical points which are *typically* AdS saddle points.

5.5.2 Uplifting a supersymmetric sector

As we discussed in section 5.3.2, generic uplifting mechanisms require the existence of a supersymmetric minimum for the uplifted critical point to be stable. The fact that there is no region of parameter space where supersymmetric AdS minima are the typical critical point does not imply that they do not exist. Supersymmetric minima require an atypical fluctuation of the smallest fermion mass, $m_1 \geq 2$, cf. eq. (5.3.12). Although in [209] it is argued that metastability is a relatively mild constraint, the probability of such fluctuation is exponentially suppressed [212, 233]:

$$\mathbb{P}(m_1 > 2) \sim e^{-\frac{8N^2}{m_h^2}}. \quad (5.5.5)$$

This result implies that when $m_h \lesssim N$, the vacua obtained using standard uplifting mechanisms will typically lead to tachyonic instabilities. For instance, if the number of fields of the supersymmetric sector is of the order of hundreds $N \sim 100$, this regime corresponds to configurations where all the chiral fermions are lighter than about a hundred times the mass of the gravitino, $m_\lambda \lesssim 100$ in our units. Nevertheless, as argued in [212], when the masses of the fermions are typically much larger than the gravitino, $m_h \gg N$, the AdS vacua are typically tachyon-free and thus they are good candidates to construct stable dS vacua using an uplifting mechanism.

As we will now discuss in detail, the results of studying the stability of a supersymmetric sector in isolation no longer hold when it is embedded in a larger model where supersymmetry is already broken. Indeed, the couplings between supersymmetric and non-supersymmetric sectors can stabilise the tachyons which appear when the supersymmetric sector is considered alone. The possibility of such an effect was discussed in detail in the context of F -term uplifting mechanisms consistent with the supersymmetric truncation of the supersymmetric sector, [83, 84].

5.6 Stability of non-supersymmetric configurations

As explained in section 5.3.3, moving away from the supersymmetric limit $\gamma = -1$ introduces a rich phenomenology, but more importantly, it is essential to describe inflation and the present vacuum, both needing a stable dS configuration. In this

5.6. Stability of non-supersymmetric configurations

section we study the probability that uplifting AdS critical points results into stable dS critical points by making use of random matrix theory techniques explained in section 5.4.2. We will argue that the presence of a supersymmetric sector imposes restrictions on the type of couplings that can give rise to these stable configurations. These restrictions appear as bounds on the geometry of the field target manifold. Furthermore, we will derive the supersymmetric mass spectrum for well motivated scenarios in which the heavy sector of the theory is consistently truncated in a supersymmetric way, as described in detail in section 5.4.1.

Already in section 5.3.3 we found necessary conditions for the metastability of non-supersymmetric configurations, and we have seen that not only the projection of the Hessian along the sGoldstino direction imposes constraints [194, 224–226], but also the presence of a supersymmetric sector might help or not in the stability of uplifted dS configurations, as shown in Figs. 5.2 and 5.6. We shall also see that these constraints can be applied not only to dS vacua, but also to inflation, where additional conditions must be satisfied [3, 195, 234].

5.6.1 Separable Kähler function

The simplest class of theories consistent with the supersymmetric truncation of the heavy sector at a configuration H_0^α are characterised by separable Kähler functions of the form [82–85]

$$G(H, \bar{H}, L, \bar{L}) = G_h(H, \bar{H}) + G_l(L, \bar{L}), \quad \text{with} \quad \partial_\alpha G_h|_{H_0} = 0. \quad (5.6.1)$$

In these theories the Kähler manifold has a cross-product structure $\mathcal{K} = \mathcal{K}_h \otimes \mathcal{K}_l$, and the reduced manifold, \mathcal{K}_l , is clearly a totally geodesic submanifold. When the Kähler manifold has this cross-product structure, the stability analysis is particularly simple, since all the bisectional curvatures of the heavy sector are zero $B[X, \lambda] = -R_{X\bar{X}\alpha\bar{\alpha}} = 0$, as well as the matrix $\nabla_X \mathcal{M}_h$, and thus the Hessian matrix has the structure discussed in section 5.3.3. Written in terms of the Hessian of the gravitino mass \mathcal{G} , it reads:

$$\mathcal{H}_h = \mathcal{G}(\mathcal{G} + 3\gamma \mathbb{1}). \quad (5.6.2)$$

The scalar mass eigenvalues are given by (5.3.15). Proceeding as in the previous section, we can also calculate the eigenvalue density function for the scalar masses after the uplifting. First, by inverting (5.3.15) we can find an expression for the fermion masses m^2 in terms of the eigenvalues of the Hessian μ^2 . The two branches read:

$$m_\pm^2(\mu) = \left[\frac{1}{2}(3\gamma + 2) \pm \sqrt{\mu^2 + \frac{9}{4}\gamma^2} \right]^2, \quad \left| \frac{dm_\pm^2}{d\mu^2} \right| = \frac{|m_\pm|}{\sqrt{\mu^2 + \frac{9}{4}\gamma^2}}. \quad (5.6.3)$$

As in the previous section, we use the Marčenko-Pastur law (5.4.9) and substitute it in (5.5.4) to find the eigenvalue density function of the scalar masses. Illustrative examples of the mass distribution are given in Fig. 5.5.

Stability of non-supersymmetric Minkowski vacua

For de Sitter vacua with a small cosmological constant $\gamma \approx 0$, the Hessian of the supersymmetric sector has a very simple expression

$$\mathcal{H}_h = \mathcal{G}^2 \quad \implies \quad \mu_{\pm\lambda}^2 = (m_\lambda \pm 1)^2, \quad (5.6.4)$$

from which is clear that the supersymmetric sector is always stable, with possible zero-modes whenever the function G has a flat direction, i.e. for each fermionic mass satisfying, $m_\lambda = 1$. In the case $m_h < 1$, the spectral density of the scalar masses resembles the Wigner's semicircle law, and the maximum fermion mass is always smaller than the gravitino mass $m_\lambda|_{\max} < 1$. Therefore, typical critical points do not present zero-modes and, moreover, the spectrum of masses of the scalar fields presents a gap, that is, the masses are bounded below by a positive value

$$\mu^2|_{\min} = (m_h - 1)^2 < 1. \quad (5.6.5)$$

Note that in this type of models the lightest scalar field of the supersymmetric sector is lighter than the gravitino. When $m_h > 1$ the spectral density has a closer shape to the Marčenko-Pastur law, and the spectrum typically contains zero-modes.

This case is particularly interesting since it corresponds to Type IIB flux compactifications at tree level, before including loop and non-perturbative corrections. In that case we can identify the (supersymmetric) H -sector with the set of complex structure and dilaton fields, while the (non-supersymmetric) L -sector would correspond to the set of Kähler moduli. In particular, due to the no-scale structure of the Kähler sector one has $G^{(L)|i\bar{j}} G_i^{(L)} G_{\bar{j}}^{(L)} = 3$, and therefore, when the complex structure and dilaton fields are fixed at a supersymmetric critical point of the potential, we have $\gamma = 0$, that is, a non-supersymmetric Minkowski vacuum, which is precisely the case at hand.

Stability of the supersymmetric sector during inflation

During inflation we have $\gamma > 0$, the size depending on the particular inflationary model under consideration. For instance, for inflationary models based on the standard KKLT construction, the stability of the volume modulus requires the Hubble parameter to be at most of order of the gravitino mass, $\gamma \lesssim 1$ [235], however there are modifications of this framework which allow for values of the Hubble parameter much larger than the gravitino mass $\gamma \gg 1$ [236].

5.6. Stability of non-supersymmetric configurations

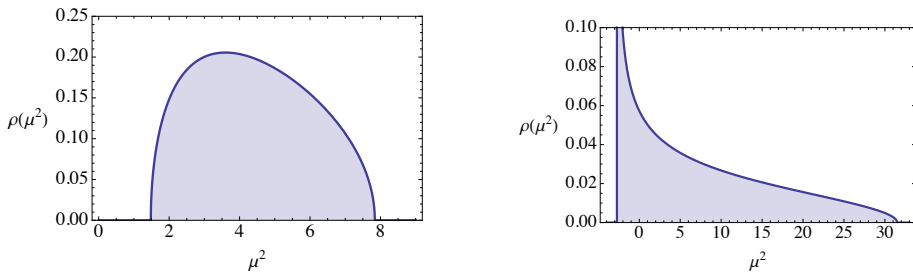


Figure 5.5 – Probability density function $\rho(\mu^2)$ for the mass spectrum after an uplifting consistent with the supersymmetric truncation of the moduli sector. The masses are measured in units of the gravitino mass. *LEFT*: When the standard deviation of fermionic masses is small, i.e. $m_h \leq m_{3/2}$, the typical configuration of the truncated sector contains no tachyons (in the plot $m_h = 0.6$, $\gamma = 1.1$). *RIGHT*: When the standard deviation of fermionic masses satisfies $m_h \geq m_{3/2}$, the typical mass spectrum of truncated fields H_0^α contains tachyons, and it is thus unstable (in the plot $m_h = 3.2$, $\gamma = 1.1$).

It can be seen from (5.3.16) that only for configurations with all the fermion masses smaller than the gravitino mass, the scalar spectrum is free of tachyons. If the standard deviation of fermion masses is larger than the gravitino mass, the spectrum will necessarily contain tachyons (except for exponentially suppressed configurations that we describe below). Recall that those configurations correspond to AdS maxima in the supersymmetric limit $\gamma \rightarrow -1$. The typical mass spectrum for $m_h < 1$ is displayed in the left plot of fig. 5.5. It can be seen that the mass of the lightest scalar field in those configurations is bounded below by

$$\mu_{\lambda}^2|_{\min} = (m_h - 1)(m_h - (3\gamma + 1)). \quad (5.6.6)$$

This is quite interesting, since it implies that the corresponding mass gap becomes wider the higher the value of the Hubble parameter, implying that for $\gamma \gg 1$ it becomes very unlikely that one of these configurations becomes tachyonic during inflation. Nevertheless, in this limit the typical mass of the lightest scalar field is still of order of the Hubble parameter H (that is, $\mu^2 \sim \gamma$), implying that there might be situations where is not possible to neglect fluctuations of the fields of the truncated sector during inflation.

In those cases when $m_h > 1$, the fermion with the largest mass is typically heavier than the gravitino and the configuration of the supersymmetric sector H_0^α is unstable, see right plot in fig. 5.5. Let us point out the difference with respect to the results in AdS of the previous section: here the Wigner-type spectra correspond to minima, while the Marčenko-Pastur type always contain tachyonic directions, as opposed to the behaviour for supersymmetric vacua. When $m_h > 1$, there might still be an exponentially suppressed fraction of configurations H_0

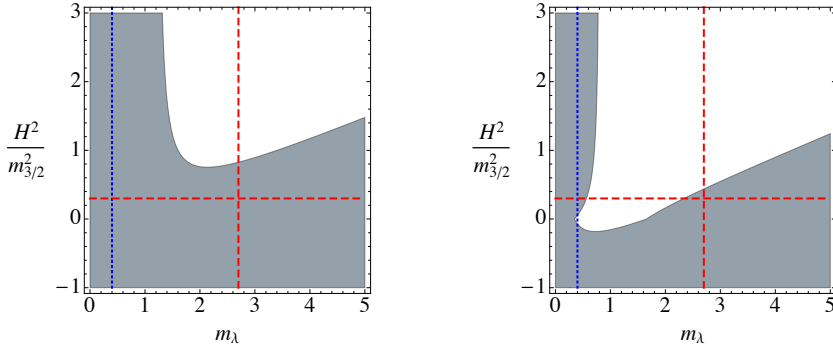


Figure 5.6 – Stability diagram of a field configuration H_0^α of the supersymmetric sector for a general Kähler function satisfying (5.4.1). The grey area is the region where the necessary conditions for stability (5.3.8) are satisfied. The vertical lines correspond to two different values of the mass scale of the truncated sector with $m_h = 0.4$ (blue dotted), $m_h = 2.7$ (red dashed), and the horizontal line to $\gamma = 0.3$. In both diagrams $\partial m_\lambda / \partial X = 0.1$, while the maximum value of the bisectonal curvatures is set to $B = 0.2$ (left plot) and $B = -0.2$ (right plot).

where the H -sector remains stable. Indeed, it follows from (5.3.16) that atypical configurations where either the heaviest fermion is lighter than the gravitino $m_\lambda|_{\max} < 1$, or the mass of the lightest fermion satisfies $m_\lambda|_{\min} > 3\gamma + 1$, remain tachyon-free. The probability of those fluctuated spectra can be estimated to leading order in $1/N_h$ and they read (see appendix D):

$$\mathbb{P}(m_\lambda|_{\min} > 3\gamma + 1) \sim e^{-\frac{2(3\gamma+1)^2}{m_h^2} N_h^2} \quad , \quad \mathbb{P}(m_\lambda|_{\max} < 1) \sim e^{-\frac{1}{6}|x|^3 N_h^2} \quad , \quad (5.6.7)$$

where $x \equiv -1 + m_h^{-2}$. Note that, in general, the Hubble parameter (and thus γ) will vary during inflation, especially at the end of the slow-roll stage. Therefore, in simple models with a separable Kähler function (5.6.1), a point representing the configuration H_0^α on the stability diagram of fig. 5.1 will move vertically as a reflection of the inflationary trajectory, as we have seen in chapter 4. The different possibilities in the simplest case where the supersymmetric sector contains a single field were studied in [3].

Let us emphasise that in a broad region of the parameter space, the most stable configurations during inflation are those where the fermionic mass spectrum is fully contained within smaller values than the gravitino mass, that is, those that correspond to minima of the gravitino mass.

5.6. Stability of non-supersymmetric configurations

5.6.2 Quasi-separable Kähler function

There are certain situations in which the terms of the Hessian (5.4.5) spoiling the separable structure, $\nabla_X \mathcal{M}$ and \mathcal{R} , become subdominant, and one can write

$$G(H, \bar{H}, L, \bar{L}) = G^{(h)}(H, \bar{H}) + G^{(l)}(L, \bar{L}) + \epsilon G_{int}(H, \bar{H}, L, \bar{L}), \quad (5.6.8)$$

with $\epsilon \ll 1$. Therefore the mass spectrum can be calculated to leading order in perturbation theory (see appendix C for details), and the necessary conditions for stability (5.3.8) become sufficient. As we will see, this class of couplings have a remarkable property: in a large region of parameter space all vacua remain stable after the uplifting to dS, including those coming from supersymmetric vacua with BF-allowed tachyons. In Fig. 5.2 we have plotted the stability diagram for a particular eigenspace h_λ with four different choices of the parameters. The grey and light blue areas represent, for different choices of $\partial m_\lambda / \partial X$ and $B[X, \lambda] = -R_{X\bar{X}\lambda\bar{\lambda}}$, the region of parameter space where the necessary conditions (5.3.8) are satisfied. Note that, as in the separable case, the minima of the gravitino mass, i.e. when $m_\lambda \leq 1$, still have better stability properties than any other field configuration when $H \gg m_{3/2}$, i.e. for $\gamma \gg 1$, which is relevant for inflation.

The stability diagrams signal the regions of the parameter space where the stability conditions are met. Now, since the horizontal axis describes *one* of the masses of the supersymmetric sector, it is important to take into account that when we describe *distributions*, with $m_h = m_\lambda|_{\max}$, all the masses of the supersymmetric sector are distributed according to the Marčenko-Pastur law along the interval $[0, m_h]$. Therefore, if there is a white region between 0 and m_h for a given γ , our scalar spectrum will contain tachyons, even if a configuration (m_h, γ) falls within the grey region. This is illustrated by the red vertical dashed line in the right plot of Fig. 5.6. A possible loophole to this argument is that of atypical fluctuated fermionic spectra such that all the fermionic masses are contained within a region that remains stable, but as we argued before, in this setup those configurations are exponentially suppressed.

As we discussed in previous sections, the bisectonal curvature is zero in KKLT constructions since the moduli space has a direct product structure for the complex structure and Kähler sectors, and is naturally suppressed in Large Volume Scenarios. For the latter type of models, the deviations of the Hessian from the separable case, which are given by the derivative of the fermion mass matrix and the curvature term, are suppressed by powers of volume.

5.6.3 Non-separable Kähler function

In this section we will consider the stability analysis of the truncated sector for a general Kähler function satisfying the condition (5.4.1) for the supersymmetric

Perturbative stability along the supersymmetric directions of the landscape

truncation of the heavy sector. In this situation the Hessian of the scalar potential along the supersymmetric sector reads

$$\mathcal{H}_h = \mathcal{G}(\mathcal{G} + 3\gamma \mathbb{1}) + \sqrt{3(\gamma + 1)} \nabla_X \mathcal{G} - 3(\gamma + 1)\mathcal{R}. \quad (5.6.9)$$

The parameters $\mu_{\pm\lambda}^2$ can no longer be identified with the squared-masses of the scalar fields of the supersymmetric sector. Therefore, the conditions (5.3.8) are necessary but not sufficient to guarantee the stability of the supersymmetric sector.

In generic situations the bisectonal curvatures will take any value, but if the Kähler manifold is regular at H_0 , the bisectonal curvatures will normally be bounded, $B[X, \lambda] \in [B_{\min}, B_{\max}]$, for all $\lambda = 1, \dots, N_h$. The bound on the bisectonal curvature (5.3.9) depends on the fermion mass, which in principle can take values between 0 and m_h . Since it must be satisfied for all the fermion masses in the distribution, let us impose it for the most restrictive one, which is $m_\lambda = 0$. In that case the bisectonal curvature is constrained by the following bound:

$$B_{\max} \geq -\frac{3\gamma + 1}{3(\gamma + 1)}. \quad (5.6.10)$$

Let us consider this bound in physically relevant situations: almost Minkowski vacua and during inflation. A summary of the bounds can be seen in Tab. 5.1.

Non-supersymmetric Minkowski vacua

For $\gamma \simeq 0$ the Hessian reads

$$\mathcal{H}_{susy} = \mathcal{G}^2 + \sqrt{3} \nabla_X \mathcal{G} - 3\mathcal{R} \Rightarrow \mu_{\pm\lambda}^2 = (m_\lambda \pm 1)^2 + \sqrt{3} \frac{\partial m_\lambda}{\partial X} + 3B[X, \lambda] \geq 0. \quad (5.6.11)$$

First, we know that the present vacuum is described by a small and positive cosmological constant, $\gamma \simeq 0$, so from (5.6.10):

$$B_{\max} \geq -\frac{1}{3} \quad (\text{dS vacuum}) \quad (5.6.12)$$

Regarding stable dS vacua, we have seen that small perturbations in the bisectonal curvature or derivatives of the masses can cause instabilities or, on the contrary, can improve the stability. In particular, if the parameters satisfy

$$\frac{1}{\sqrt{3}} \sigma_D \leq B_{\min}, \quad (5.6.13)$$

the necessary stability conditions (5.3.8) are satisfied by typical vacua, but any other case requires a case by case analysis. For example when $\partial m_\lambda / \partial X > 0$ and $B[X, \lambda] < 0$, uplifting to stable dS vacua strongly constrains m_h to small values, to the point that for $B[X, \lambda] < -1/3$ the only (exponentially suppressed) hope is to have an atypical fluctuated fermionic spectrum such that all the masses fall on the stable region.

5.7. Conclusions

$H \ll m_{3/2}$ (Dark energy)	$H \approx m_{3/2}$ (Inflation)	$H \gg m_{3/2}$ (Inflation)
$B_{\max} \geq -\frac{1}{3}$	$B_{\max} \gtrsim -\frac{2}{3}$	$B_{\max} \gtrsim -1$

Table 5.1 – Necessary conditions for the stability of a typical configuration of the supersymmetric sector. B_{\max} is the maximum value that can be attained by the bisectonal curvature at (H_0^α, L_0^i) varying the s Goldstino direction z_X , and the direction of the fermion mass eigenstate z_λ .

Stability of the supersymmetric sector during inflation

Another interesting limit is $H \gg m_{3/2}$, or in other words $\gamma \gg 1$, which is relevant for inflation. In those cases we have the following necessary conditions:

$$H \approx m_{3/2} : \quad B_{\max} \geq -\frac{2}{3}, \quad H \gg m_{3/2} : \quad B_{\max} \geq -1 \quad (5.6.14)$$

When the parameters satisfy

$$m_h \leq 1 + B_{\min} \quad (5.6.15)$$

all the stability constraints (5.3.8) are satisfied by the supersymmetric sector, and thus with probability $P \sim \mathcal{O}(1)$ the supersymmetric sector will remain tachyon-free along the inflationary trajectory. Other situations have to be studied in a case by case basis.

In order for the fluctuations of the supersymmetric sector to be suppressed during inflation with $\gamma \approx 1$ we would have the slightly tighter constraint $B_{\max} \geq -1/2$.

5.7 Conclusions

In this chapter we have extended the analysis of chapter 4 in several aspects. Our results illustrate, in a different context that chapters 2 and 3, the importance of considering the coupling between different sectors of the theory. In this chapter we have studied the type of coupling that is necessary for the stability of a supersymmetric sector which is embedded in a theory with broken supersymmetry. This case falls outside the scope of previous analyses. In particular we have considered $\mathcal{N} = 1$ supergravity models involving only chiral multiplets, and which are consistent with the supersymmetric truncation of the fields preserving supersymmetry. This class of theories is characterised by a Kähler function G satisfying:

$$\partial_\alpha G(H, \bar{H}, L, \bar{L})|_{H_0} = 0 \quad \text{for all } L^i,$$

where L^i are the fields in the supersymmetry breaking sector, and H^α are the fields in the supersymmetric sector which are frozen at a configuration H_0^α . In addition, following [211, 212], we have treated the couplings in the decoupled (supersymmetric) sector as random variables, and we studied the Hessian of the scalar potential using tools from random matrix theory. This analysis is motivated by the supergravity description of the dilaton and complex structure moduli in KKL_T constructions and Large Volume Scenarios of type-IIB flux compactifications, where the complex structure and dilaton fields are truncated from the theory before considering the stability of the Kähler moduli, and the truncation is done in a way that leaves supersymmetry approximately unbroken. The stability of the truncated sector is crucial to ensure the viability of cosmological models based on supergravity theories with this structure, both when they describe the present vacuum with a small cosmological constant (dark energy), as well as for scenarios of slow-roll inflation. The main conclusion of our analysis is that, in a broad range of parameters, the configuration of a decoupled supersymmetric sector H_0^α remains free of tachyons with order one probability, $\mathbb{P}_{\text{stable}} \sim \mathcal{O}(1)$.

In order to perform the analysis we have derived the set of necessary conditions (5.3.8) for the stability of the supersymmetric sector. These conditions, which can be seen as constraints on the Kähler potential K and the superpotential W , are expressed in terms of the ratio of the Hubble parameter to the gravitino mass ($\gamma = H^2/m_{3/2}^2$), the masses the chiral fermions and their derivatives along the sGoldstino direction (m_λ and $\partial m_\lambda/\partial X$, respectively), and the bisectonal curvatures of the Kähler manifold

$$B[X, \lambda] \equiv -R_{I\bar{J}K\bar{L}} z_X^I \bar{z}_X^{\bar{J}} z_\lambda^K \bar{z}_\lambda^{\bar{L}}.$$

Here $R_{I\bar{J}K\bar{L}}$ are the components of the Riemann tensor, z_X is a unit vector along the sGoldstino direction, and the z_λ form an orthonormal basis on the supersymmetric sector. In general, the conditions (5.3.8) are necessary but can not guarantee the stability of the truncated supersymmetric sector. Still, assuming that the number of H^α fields is large, $N_h \gg 1$, and that there is no large hierarchy between the masses in the truncated sector and the supersymmetry breaking scale (as in LVS), we were able to derive generic constraints on the geometry of the moduli space. In particular, we have shown that positive values of the bisectonal curvatures $B[X, \lambda]$ considerably improve the stability of the supersymmetric sector, as is summarised in Table 5.1.

We have analysed in detail a class of models which includes physically relevant scenarios, and for which the conditions (5.3.8) are *necessary and sufficient* for the stability of the supersymmetric sector. This also allows us to perform a detailed study of the scalar mass spectrum and establish specific criteria to achieve tachyon-free spectra. This class of models is characterised by an almost separable Kähler function:

5.7. Conclusions

$$G(H, \bar{H}, L^i, \bar{L}) = G_h(H, \bar{H}) + G_l(L, \bar{L}) + \epsilon G_{mix}(H, \bar{H}, L, \bar{L}),$$

$$\text{with } \partial_\alpha G_h|_{H_0} = \partial_\alpha G_{mix}|_{H_0} = 0 \quad \text{and} \quad \epsilon \ll 1.$$

When the parameter ϵ is set to zero, this type of Kähler function describes a large class of no-scale models, and in particular it includes the effective supergravity description of type-IIB compactifications to zero-order in α' and non-perturbative corrections. In the latter case the fields H^α are identified with the dilaton and complex structure moduli, and L^i with the Kähler sector. When ϵ is small but non-zero, this type of theories include models with a similar structure to the effective description of LVS, where the magnitude of ϵ is suppressed by the volume of the compact space, $\epsilon \sim 1/\mathcal{V}$. We have then studied case by case the typical scalar mass distribution of the supersymmetric sector and its dependence on the parameters appearing in (5.3.8). A fundamental quantity that determines the stability of field configurations is the mass scale of the supersymmetric sector in units of the gravitino mass, denoted by m_h . This parameter is defined in such a way that typically the fermion masses are distributed in the interval $m_\lambda \in [0, m_h]$. When the mass scale of the supersymmetric sector is larger than the gravitino mass, $m_h > 1$, the typical spectrum has the following general features:

- At Minkowski vacua the spectrum has no tachyons in the fully separable case ($\epsilon = 0$). However, depending on the parameters, the scalar mass spectrum may contain a significant fraction of fields which can be much lighter than the gravitino.
- Minkowski configurations are very susceptible to become tachyonic when the Kähler function has a small non-separable term, for instance with $\epsilon \sim \mathcal{O}(10^{-1} - 10^{-2})$. However, in LVS the parameter $\epsilon \sim 1/\mathcal{V}$ is exponentially small, and in practice we recover the fully separable case, for which Minkowski vacua are metastable.
- In the regime $m_h \sim \mathcal{O}(1 - 10^2)$, typical field configurations always become tachyonic for sufficiently large values of the ratio $\gamma = H^2/m_{3/2}^2$.
- When the mass scale m_h is much larger than the gravitino mass, $m_h \gg N_h \gg 1$, the supersymmetric sector is always stable. This is precisely the hierarchy needed in KKLT type of stabilisation mechanisms.

Conversely, when the mass scale of the supersymmetric sector is smaller than the gravitino mass, $m_h < 1$, the spectrum displays a mass gap which protects the stability of the truncated sector. Therefore, provided the non-separable corrections to the Kähler function are small, *the truncated sector is typically stable in the regime $m_h < 1$, regardless of the ratio $H/m_{3/2}$* . Interestingly, in this regime, the configuration of the supersymmetric sector always corresponds to minima of the Kähler function G . The presence of the mass gap in the spectrum suggests that the robust stability properties of the minima of G will survive

in more realistic models where the truncation of the supersymmetric sector is only approximate. Therefore, the minima of the Kähler function can be of interest in exploring new stabilisation mechanisms, for example in cases where the supersymmetric sector is not protected by a large mass hierarchy, as in KKLТ constructions, or where the non-separable corrections in the Kähler function are small but not exponentially suppressed as in Large Volume Scenarios.

From our analysis it follows that, in general, *supersymmetric AdS minima are more difficult to realise than the stabilisation of a supersymmetric sector*, when this sector is embedded in a theory where supersymmetry is spontaneously broken. In other words, a decoupled supersymmetric sector can be stabilised at configurations which do not correspond to supersymmetric minima in the absence of supersymmetry breaking. This discussion already allows us to understand the situation in LVS in relation to the random supergravity analysis that we have performed here and the one in [212]. Recall that in LVS all moduli can be stabilised in a very model-independent way, while the fraction of configurations of the complex structure moduli which correspond to supersymmetric minima of the potential induced by fluxes is exponentially small $\mathbb{P}_{\text{susy}} \sim \exp(-8N_h^2/m_h^2)$ [212]. Conversely, our results indicate that there can be a large fraction of stable configurations for the supersymmetric moduli when the supersymmetry breaking effects are included, $\mathbb{P}_{\text{stable}} \sim \mathcal{O}(1)$. This can be easily understood from the discussion in the previous paragraph: by considering only supersymmetric AdS minima of the scalar potential induced by the fluxes, we are discarding most configurations where the supersymmetric sector is stable. Actually, *the non-generic couplings between the supersymmetric sector and the remaining moduli can turn all the Breitenlohner-Freedman allowed tachyons of supersymmetric critical points into stable modes*. In Large Volume Scenarios the no-scale structure of the Kähler sector is fundamental in order to achieve the stabilisation of the supersymmetric moduli.

Many interesting questions regarding the implications for inflation in supergravity arise from our analysis. In particular, it is important to understand which situations lead to a supersymmetric sector with a scalar mass distribution where all the scalar field masses remain much larger than the Hubble scale, since this would describe a stable supersymmetric sector with suppressed isocurvature fluctuations. It would also be useful to study the inflationary constraints in particular models where inflation is driven by a field orthogonal to the sGoldstino direction, or in other words, a field contained in the supersymmetric sector, as in [86]. Last, it is interesting to understand why there is an optimum negative value for $\partial m_\lambda / \partial X$ that optimises the stability, as well as the effect of this term in the scalar spectral density and its physical interpretation.